Electrochemically instantaneous reduction of conducting polyaniline-coated latex particles dispersed in acidic solution

Electrochemically instantaneous reduction of conducting polyaniline-coated latex particles dispersed in acidic solution

Han Chen, Jingyuan Chen, Koichi Aoki[*], Toyohiko Nishiumi

Department of Applied Physics, University of Fukui, 3-9-1 Bunkyo, Fukui-shi,

910-8507 Japan

Abstract

A cathodic voltammetric wave was observed in an aqueous suspension of mono-dispersed, spherical polyaniline-coated polystyrene particles, whereas no anodic wave was detected. This irreversibility was common to particles with eight different diameters ranging from 0.2 to 7.5 μm. Such irreversibility cannot be found at polyaniline-coated electrodes, and thus is a property of the dispersion of polyaniline latex. The reduction current was controlled by diffusion of dispersed particles. The reduction, being the conversion from the electrical conducting state to the resistive one, should begin at a point of contact between the conducting particle and the electrode in order to be propagated to the whole particle rapidly. In contrast, the oxidation proceeds slowly with the propagation of conducting zone, during which Brownian motion lets the particle detach from the electrode. The number of loaded aniline units per particle, determined by weight analysis, ranged from 6×10^6 ($^\phi 0.2$ μm) to 3×10^{11} ($^\phi 7.5$ μm) and was proportional to 2.9 powers of the particle diameter. The diffusion-controlled current of the cathodic wave was proportional to 2.4 powers of the diameter. The difference in these powers, 0.5, agreed with a theoretical estimation of the diffusion-controlled current, the diffusion coefficient for which was given by the Stokes-Einstein equation.

Key words: polyaniline, suspension of redox latex particles, voltammetric diffusion-controlled current, core-shell structure, irreversibility

---

[*] e-mail kaoki@u-fukui.ac.jp, tel +81-90-8095-1906, fax +81-776-27-8494 (K.A.)

1. Introduction

Redox latex particles are macromolecules with functionality arising from redox moieties. They can make up uniform polymeric films with large areas by being spread on electrodes [1,2]. Redox latex particles have exhibited the following: anti-corrosive properties [3,4], strong catalytic activity of O_2, H_2O_2, trichloroacetic acid and NO_2^- by core-shell polystyrene-hemoglobin particles [5], and a pair of well-defined reversible peaks of Fe^{III}/Fe^{II} for by hemoglobin-coated particles [6]. When redox latex particles are dispersed in solution as colloidal suspensions, they can be regarded as jumbo redox particles, and serve as models of metal nanoparticles, enzymes and living cells. Acid-substituted polystyrene sulfonate latex suspensions have worked as jumbo redox particles for reduction of the hydrogen ion [7,8] in order to confine the hydrogen ion to the latex core as colloidal crystals [9,10]. Ferrocene-immobilized latex particles have brought about partial electron transfer between the redox sites of the particles and an electrode depending on the particle size [11-13]. Suspensions of hemin-immobilized polyallylamine-polystyrene latex have shown greater catalytic reduction activity for dioxygen [14] and carbon dioxide [15] than molecular hemin has. Potential cycling of polypyrrole latex has varied the degree of adsorption of imidazole [16] to the latex. Polyaniline latex suspensions have exhibited discretized currents at microelectrodes [17].

A common feature of voltammograms for dispersed jumbo redox particles is the diffusion-controlled mass transport of the particles, which has been demonstrated by the proportionality of voltammetric peak currents to the square root of potential scan rates [7-9,11-14]. One particle usually has more than 10^5 redox sites or exchanged electrons. The voltammetric behavior of jumbo redox particles is quantitatively different from that of conventional redox particles for the following two reasons:

(A) The peak current of a simultaneous n-electron reaction is known to be proportional to $n^{3/2}$ [18-20]. However, the peak current of jumbo particles with n-redox molecules

each being composed of one-electron reactions is proportional to n [21].

(B) All the redox sites of one particle do no react electrochemically as the particle becomes large. This phenomenon is called "partial charge transfer" [11-13]. Possible reasons for the loss of reactivity are a small area of contact between the redox particle and the electrode [11-13] and a loss of local hydrophilicity as for vinylferrocene films [22-24]. The percentages of redox sites that are active are increased by rotation of reacting particles on an electrode [11] or in suspensions [13,25].

A strategy for making latex redox sites react completely is to use conducting polymers in the electrical conducting state, which can keep the whole particle of equal potential. When the conducting polymeric particle comes into contact with the electrode, it acquires the same potential as the electrode. Then the electrode reaction occurs over the entire particle, and hence the reduction for the conducting-to-insulating conversion is so rapid as to be controlled by the supply of dopant until the path of any conducting site to the electrode is cut off by electric percolation [26-29]. However, the electrochemical oxidation for the insulating-to-conducting conversion is controlled by the propagation of the conducting zone [30] at the velocity of ca 1 mm s^{-1} in dopant-rich solutions [31-34], and is slower than the reduction. This slow oxidation is expected to exhibit the size-dependence of partial electron transfer. This manuscript reports the voltammetric conversion of polyaniline-coated polystyrene latex particles dispersed in aqueous acid solution in order to find not only a relationship between the partial reaction and particle size, but also the irreversibility of the conversion.

2. Experimental

2.1. Chemicals

Poly(n-vynylpyrrolidone) (PVP) (Wako，360 kg mol^{-1}) was used to stabilize the

polymerization of styrene. Ammonium peroxydisulfate (Wako), aniline hydrochloride (Kanto), α-azoisobutyronitrile (AIBN) (Kanto), ethanol (Wako), methoxyethanol (Wako), ferrocene (Kanto), potassium chloride (Nacalai Tesque), potassium nitrate (Wako) and sodium dodecylsulfonate (SDS) were used as received. All aqueous solutions were prepared with deionized and twice-distilled water.

200 cm^3 Styrene was rinsed with 50 cm^3 5% NaOH five times to remove inhibitors. The color of the first rinse was red-brown, and that of the second one was yellow. The styrene became colorless after the third and subsequent rinsings. The styrene was rinsed with 50 cm^3 tap water for five times to remove NaOH. Subsequently, it was rinsed with 50 cm^3 distilled water three times. Anhydrous $CaCl_2$ was added for half a day to remove water. The styrene was distilled under low pressure, and stored in a refrigerator before use.

2.2. Controlled synthesis of given-sized polystyrene latex

Seed particles were prepared by the dispersion polymerization of styrene under various conditions depending on particle size. For example, 1.5 g PVP was added to a mixture of 40 cm^3 ethanol and 36 cm^3 methoxyethanol in a three-necked round-bottomed flask. 15 cm^3 Styrene was added to the mixture, including 0.33 g AIBN, a radical initiator. The polymerization was performed under a nitrogen atmosphere at 70 ^oC with mechanical stirring at 160 rpm for 24 h. The resulting latex was centrifuged and re-dispersed three times with 1% PVP in water. This process generated uniformly-sized spherical particles 1.08 μm in diameter. The size of polystyrene particles was controlled with concentrations of styrene, radical initiator (AIBN) and steric stabilizer (SDS or PVP), and with the stirring speed. The conditions are summarized in Table 1.

2.3 Coating polystyrene with polyaniline

Aniline hydrochloride (8 mmol) was added to 100 cm^3 of 4% (w/v) suspension of

polystyrene latex. The mixture was stirred in an ice bath for 2 h in order to adsorb aniline onto the surface of the latex. Polymerization was performed by adding 2.45 g ammonium persulfate (oxidant) to the mixture, which was stirred for 5 h at 0 $^{\circ}$C and for a further 14 h at room temperature. The color of the suspension changed from white to dark-green. The suspension was sedimented in a refrigerated centrifuge, SRX-201 (TOMY, Tokyo), to prevent degradation of polyaniline [35]. The centrifugation separated the mixture of the product into three layers. The middle layer contained fragments of polyaniline. The bottom layer, which contained a high proportion of the polyaniline-coated latex, was re-dispersed in 0.5 M sulfuric acid including 1% PVP, and then was centrifuged. The re-dispersion and centrifugation were iterated several times until the top layer (water) became clear.

The concentration of particles in a suspension was determined by drying and weighing a sample volume of the suspension. The weight was converted into the volume with the density of PS (1.05 g cm^{-3}) on the assumption that the polyaniline film was very thin. The division of the sample volume by the volume of one particle ($4\pi r_L^3/3$; r_L radius) yielded the number of particles in the aliquot.

2.4. Measurements and instrumentation

Cyclic voltammetry was carried out with a potentiostat, Compactstat (Ivium Tech., Netherlands) in the latex suspensions including 0.5 M H_2SO_4 and 1% PVP in a conventional three-electrode cell. A Pt disk 1.6 mm in diameter (BAS, Tokyo) was used as a voltammetric working electrode. The surface of the working electrode was polished with alumina paste on wet cotton, and was rinsed with distilled water in an ultrasonic bath before each voltammetric run. A platinum wire and an Ag|AgCl electrode were used as the counter-electrode and the reference electrode, respectively. The electrochemical measurement was performed under a nitrogen atmosphere.

Digital optical photomicrographs of the latex particles were obtained with a video

microscope, VMS-1900 (Scalar), and were transferred to a PC using a MPG capture board. The size distribution and particle-dispersion were determined by a light scattering instrument (Malvern Zetasizer Nano-ZS, UK), SEM (Hitachi, S-2600H) and the video microscope.

3. Results and Discussion

3.1 Basic features of polyaniline-polystyrene latex

We know empirical rules of synthesizing size-controlled polystyrene latex: smaller particles are generated in more hydrophobic solvents for higher concentrations of the surfactant, which is SDS rather than PVP, at higher stirring speed. From a reaction-mechanistic view point, the size may be related to the droplet size in emulsions, the reaction rates of polymerization, solubility of styrene, or viscosity of the emulsions. Since these possibilities overlap, only an increase in concentration of SDS does not always produce small particles. We tried to synthesize 30 kinds of latexes and selected eight sets of conditions, given in Table 1. When the polystyrene latex was chemically coated with polyaniline, the resulting latex was composite polyaniline-polystyrene (PANI-PS) latex with the core-shell type [36]. Its suspension sedimented faster than the PS suspension.

We examined size distribution of PANI-PS particles using SEM, the optical microscope and the light scattering instrument. Figure 1 shows the size distribution (A) and an example photograph (B) from the optical microscope, which demonstrate the almost uniform particle size-distribution. Observation of the suspension with the optical microscope found no aggregation of particles, as they were in Brownian motion.

It is important to evaluate the number of redox sites of polyaniline on one particle as well as to obtain a relationship between this number and the particle size. For

quantitative determination of the amount of polyaniline, we used three techniques: weight analysis (WA) combined with dissolution, thermogravimetric analysis (TGA), and elemental analysis. For the WA, the dried latex, which was weighed in advance, was immersed in tetrahydrofuran (THF) to dissolve only the PS with PANI left as a solid [35]. The PANI residue was collected with filtration, dried and weighed. The weight ratio provided the molar ratio of PANI to PANI-PS. Figure 2 shows TGA curves of PANI-PS, PA and PS. Polystyrene began to decompose at $320^{\circ}C$ and caused depression of the temperature at $500^{\circ}C$ probably because of the endotherm before sublimation or evaporation. Polyaniline decomposed in the temperature range from 300 to $600^{\circ}C$, which overlaps the TGA curve for PS. The endotherm was observed for PS (Fig. 2(c)) but not for PANI (Fig. 2(b)). We regarded tentatively the decrease in weight before the endothermic point as PS and the decrease after the point as PANI. Table 2 lists the values of weight ratio by WA and TGA. The values by TGA were ca. 1.2 times larger than those by WA. The overestimation is ascribed to the assumption that PANI may decompose independently of PS. We adopted the values from WA for the evaluation of the number of redox (polyaniline) units. However, TGA was used routinely for evaluation of the ratio with the correction factor (1.2). In addition, elemental analysis was carried out on the expectation that the ratio of the amount of N to that of C might provide the molar ratio of PS to PANI. However, the ratio of PANI to PS by elemental analysis was larger than the values obtained by WA and TGA, probably because PVP used in the synthesis increased the content of N. Therefore, we did not use the data obtained from elemental analysis.

If the PANI film covers the PS sphere uniformly, the weight ratio of PS to PANI is equivalent to $\rho_s r_s^3 / \rho_a (r_L^3 - r_s^3)$, where r_L and r_s are radii of the latex and the PS-core, respectively, and ρ_s (1.05 g cm^{-3}) and ρ_a (1.46 g cm^{-3}) are the densities of PS and PANI, respectively. The experimental values of the weight ratios yielded the ratio of the thickness of the PANI-shell to the radius of the latex, t/r_L (= 1 - r_s/r_L), values of which are given in Table 2. We determined t, from which we evaluated the number of aniline

units per particle, m. These values are listed in Table 2.

The above calculation holds only when the PANI film is uniform. There are three kinds of non-uniformity; (i) local loss of the film on a latex surface, i.e., patchy films, (ii) combinations of thick and thin shells on one latex, and (iii) difference in film thickness on different particles, one particle having uniform film. We observed morphology and uniformity of PANI films thick enough for resolution of the optical microscope. Photographs of the cross-section of the PANI-polymerized PS films by the optical microscope showed a clear boundary between the PANI domain and the PS domain, and exhibited uniform thickness within the resolution of the microscope. The surface of the PANI film took fibril network, as is for electrochemically polymerized PANI films. The network structure supports a patchy film, i.e., there being many holes in the PANI net. However, it covers a latex sphere.

Figure 3 shows logarithmic dependence of m and t on the radii. Both data approximately fell on each line. The slopes of log m and log t vs. log r_L were 3.1 and 1.1, respectively. The proportionality of the amount of PANI per particle with the particle volume suggests a uniform distribution of PANI over the sphere rather than the core-shell structure. This suggestion is inconsistent with the core-shell structure observed by SEM after dissolution of only PS [35]. Since the volume of the thin PANI-shell is expressed approximately by $V = 4\pi r_L^2 t$, the proportionality $t = k\, r_L^{1.1}$ in Fig. 3 directly yields $V = 4\pi k r_L^{3.1}$, and vice versa. The proportionality $t = k\, r_L^{1.1}$ rather than $t = k\, r_L^{0}$ may imply suppression of the polymerization of PANI by curvature effects. We attempted to estimate the effect of the curvature by use of the Young-Laplace equation [37]. The curvature of a sphere 1 μm radius exhibits 14 m rise of water in a glass capillary. This height corresponds to 1.4 atm or 2 J mol^{-1} of water. This value is too small to change the polymerization energy (at least on the order of 10 kJ mol^{-1}), and thus the curvature effect is negligible. Another explanation of $t = k\, r_L^{1.1}$ is due to a relation between the loaded amount of aniline and that of PS latex in the synthesis. We coated the common weight of PS latex (4 g (= W_s)) with the common amount of aniline

(8 mmol (= W_a/93)) for all kinds of latex. Letting N be the number of PS particles in the reaction vessel, we obtain $N(4\pi/3)r_s^3\rho_s = W_s$ for the weight of added PS latex and $N4\pi r_s^2 t\rho_a = W_a'$ for the polymerized aniline. Taking the ratio yields $t = (\rho_s W_a'/3\rho_a W_s)\, r_s$. This is close to $t = k\, r_L^{1.1}$ because of $r_s \cong r_L$. The value of $\rho_s W_a'/3\rho_a W_s$ is 1.3, whereas the slope in Fig.3 is $k = 5.0$. Thus a quarter of the loaded amount of aniline (W_a) in the vessel participated in the formation of the PANI shell.

3.2 Voltammetry of PANI-PS suspensions

PANI-PS suspensions were dark-blue, suggesting the emeraldine form, which is in the electrically conducting state. This was supported by the open circuit potential of the suspensions of ca. 0.5 V vs. Ag|AgCl, which is more positive than the redox potential, 0.1-0.25 V, for the reaction between leucoemeraldine and emeraldine. Figure 4 shows voltammograms of the PANI-PS suspensions for $r_L = 1.08$ μm at two scan rates. Only the cathodic wave was observed at 0.05 - 0.1 V for large particles, whereas the very small anodic peak was seen for small particles at slow scan rates. This irreversibility seems strange in that a polyaniline-coated electrode in acidic solution is known to exhibit not only a broad cathodic peak but also a sharp anodic peak in the range from 0.0 to 0.25 V with common charge. The PANI particles were adsorbed on the Pt electrode in the absence of the surfactant and low concentration of the suspension [35], and thus generally have attractive interaction with the electrode. However, the particles in the present work were not adsorbed after voltammetry by a view of the microscope.

Figure 5 shows dependence of the cathodic peak current on the square-root of the scan rate, v. The proportionality implies diffusional control. There are two possibilities to explain diffusion: one being diffusion of PANI chain or dopant ions within particles adsorbed to the electrode, and the other being diffusion of particles themselves. The former should cause the current to be independent of stirring the suspension because external convection has little influence on mass transport within particles. The current

was enhanced with increased stirring. Furthermore, no adsorbed particles were observed on the electrode surface with the optical microscope before and after voltammetry. Therefore, the latter possibility is accepted; the proportionality is due to diffusion of particles. In other word, thermal fluctuation (diffusion) for the latex is predominant over interaction between particles and the electrode.

According to the theory of voltammetry for the n-electron transfer reaction, with each step being independent, the cathodic peak current is expressed by

$$I_p = -0.446 FAnc * \sqrt{DvF/RT} \tag{1}$$

where $c*$ is the molar concentration of the latex if the latex particle is to be regarded as a molecule, D is the diffusion coefficient of the particle, and A is the electrode area. Eq.(1) is different from the conventional one in that the power of n is 1 rather than 3/2 [21]. Since the reduction of PANI occurred rapidly accompanied by slight logarithmic delay [38], we regard the reduction of PANI as a reversible reaction and apply Eq.(1) for the reversible peak current. We shall focus on the dependence of the current on the radii of the particles. We temporarily regard n (the number of exchanged charge of PANI per particle) as m (the number of aniline units per particle). In order to extract only the radii-dependence of the peak current, we transposed the directly measurable variables, m, $c*$ and $v^{1/2}$ in Eq.(1) to the left hand side. Then we have

$$\left(-I_p v^{-1/2}\right)\left(mc*\right)^{-1} = 0.446 FA\sqrt{DF/RT} \tag{2}$$

Values of $I_p v^{-1/2}$ at given values of r_L and $c*$ were determined from the slope in Fig. 5 for each particle, whereas values of m are shown in Table 2. Figure 6 shows logarithmic plots of the values on the left hand side of Eq.(2) against the radii. All the values fell on a line, the slope of which was -0.48. The variable containing the radii on the right hand side of Eq.(2) is the diffusion coefficient through the form of the Stokes-Einstein equation, $D = k_B T/6\pi r_L \eta$, where k_B is the Boltzmann constant and η is the viscosity of the suspension. The diffusion coefficient should theoretically let the left hand side be proportional to $r_L^{-1/2}$. The theoretical order -1/2 is close to the experimental value (-0.48).

The agreement suggests the validity of Eq.(1) for the radii on the assumption that m is proportional to n. The radii-dependence is different from that of ferrocene-immobilized latex suspensions, in which the partial electron transfer has decreased n from m with an increase in the radii owing to geometrical restrictions on the contact area with the electrode [11-13].

We evaluated n from values of $I_p v^{-1/2}$, D, c^* and A, where values of D were determined by the Stokes-Einstein equation, as listed in Table 2. Values of n/m thus obtained were plotted against the logarithm of r_L in Fig. 7, suggesting the independence from the radii. The average value of n/m, 0.22 is much smaller than unity. This fact can be partially explained in terms of the well-known report that one of four aniline units participates in the redox reaction of emeraldine/leucoemeraldine [39] in the potential domain from 0.0 to 0.25 V. However, it is (0.22×4 = 0.88) still smaller than unity. According to the theory of propagation of conducting zones, an emeraldine film is not converted completely to leucoemeraldine by the electrochemical reduction because the electric path in the emeraldine (conducting) species is cut off by electric percolation [40]. This concept has been demonstrated by the experiment in which a quarter of the emeraldine form was left behind from reduction in the film [41]. The complete reduction had a logarithmic time dependence [42-46]. The reduction should proceed irrespective of non-uniformity of the fibril films so far as the conducting domains are connected each other.

A jumbo particle approaches to the electrode by translational diffusion accompanied by rotation. After it comes into contact with the electrode, it rotates near the electrode and may collide again with the electrode. Thus the rotation should enhance diffusion [25]. Mass transport of the present latex may include not only translational diffusion but also rotational diffusion. Since a value of the translational diffusion coefficient is close to that of the rotational diffusion coefficient, it is difficult to extract a component of rotational diffusion from the current by use of the dependence of the peak currents on the radii.

Figure 8 summarizes illustratively the predicted irreversibility of the redox reaction. (a) The PANI-PS particle with the inner potential, E_1', for the oxidation (conducting state) approaches the electrode by diffusion in the suspension. The potential of the electrode is kept to the reduction state, E_2 for PANI. (b) Immediately after it comes in contact with the electrode, the inner potential changes drastically from E_1' to E_2 all over the PANI shell due to the electrically conducting state. (c) The PANI, controlled by E_2, begins to be reduced electrochemically to the insulating state over the whole shell, involving ion transport into the shell of the particle. As the reduction proceeds, it increases the resistivity of the shell and finally ceases at up to 88 % completion as the electric percolation is cut off [41]. (c) The inner potential, E_2', of the partially reduced PANI may be more positive than E_2, because of the contribution of the oxidized species left over. (d) The particle composed of 88 % reduced species disperses to the bulk suspension. (e) When it collides with the electrode at the backward scan, it is oxidized at the potential E_1. However, only the contacting area of the shell can be oxidized at the electrode because leucoemeraldine far from the contacting point keeps the potential E_2' and is not changed to E_1 by the electrode. The ratio of the oxidized domain (the black in (e)) to the shell volume is smaller with an increase in the radii. Therefore the irreversibility is more marked for larger particles, as is consistent with our experimental results.

4. Conclusions

PANI-PS latex particles with uniform size-distribution were synthesized by adjusting amounts of surfactants and varying the stirring rate of the reaction mixture. Microscopic observation of THF-dissolved particles revealed that the latex had a core-shell type. The thickness of PANI-shell, which was evaluated by weight analysis and DTA, was approximately proportional to the radius of the particle. Although this fact seems to

suggest a uniform PANI-distribution rather than a core-shell structure, it is due to the synthetic conditions for the amount of aniline loaded and the diameter of the core. A quarter of the loaded aniline formed the PANI shell. The thickness of PANI shell was ca. 5 % of the radius.

The PANI-PS suspension showed a cathodic wave and a very small anodic wave. The cathodic current, which we ascribed to the reduction of emeraldine to leucoemeraldine, was controlled by diffusion of the suspended latex particles rather than adsorbed particles. Values of $I_p v^{-1/2}$ were proportional to $r_L^{-0.48}$. This trend was explained in terms of the proportionality of I_p to $D^{1/2}$ or $(k_B T / 6 \pi \eta r_L)^{1/2}$ through the Stokes-Einstein equation. The peak currents for various radii agree with the variation in Eq. (2). That is, n was independent of the radii, different from the voltammograms of a ferrocene-coated suspension. The reduction efficiency, as high as 80-90 %, is ascribed to the electric conducting state of PANI, the inner potential of which can equalize over the shell to the electrode potential when the particle comes into contact with the electrode. In contrast, the oxidation efficiency, as low as non-detection, is ascribed to the slow propagation of the conducting zone.

5. Acknowledgement

Figure Captions

Fig.1 (A) Size distribution of the PANI-PS aqueous suspension of particles with 0.40 μm in diameter, measured with the light scattering instrument, and (B) photograph of the suspension by the SEM.

Fig.2. TGA curves of (a) PANI-PS latex, (b) PANI and (c) PS.

Fig.3. Logarithmic variations of the number of polyaniline-units, m, and the thickness of the polyaniline-shell, t, with the radii of various PANI-PS latexes.

Fig.4 Cyclic voltammogram of 4 g dm^{-3} PANI-PS suspensions 1.08 μm in diameter including 0.5 M H_2SO_4 at the Pt electrode for at the scan rates of (a) 100 and (b) 10 mV s^{-1}.

Fig. 5. Dependence of the cathodic peak currents in the PANI-PS suspensions (a) 0.4, (b) 3.9, and (c) 7.5 μm in diameter including 0.5 M H_2SO_4 on the square-root of potential scan rate.

Fig. 6. Logarithmic variation of $I_p v^{-1/2} m^{-1} c^{*-1}$ with the radii of the particles, where X means the unit of μm V$^{-1/2}$ s$^{1/2}$ mM^{-1}.

Fig. 7. Variation of n/m with the radii of the particles.

Fig. 8. Illustration of (b)-(d) the reduction and (e) the oxidation of PANI-PS particle, where E_1 and E_2 are electrode potentials for the reduction and the oxidation of PANI, respectively, E_1' and E_2' are inner potentials for the reduction and the oxidation of PANI, respectively. The black, the white and the hatched domains stand, respectively, for the conducting species of PANI, the reduced species of PANI, and PS.
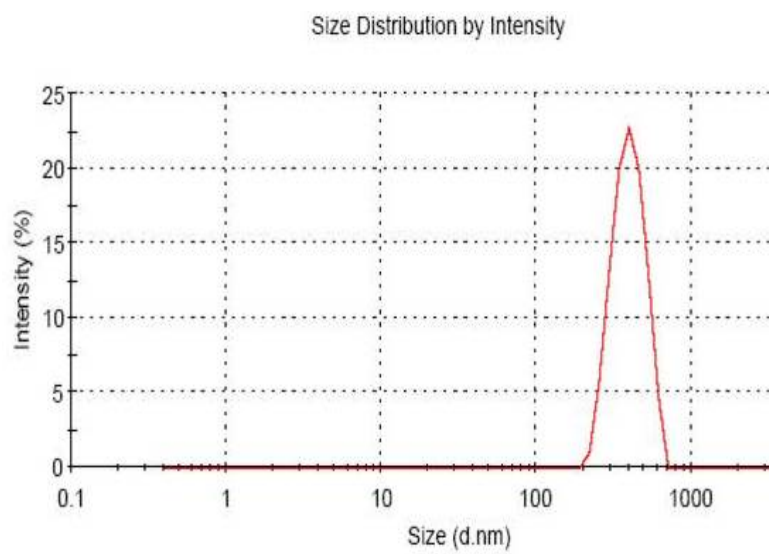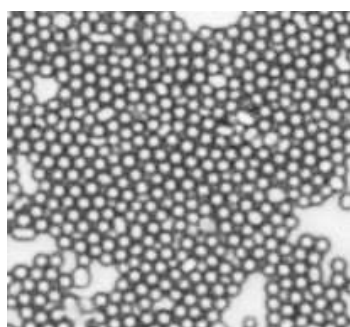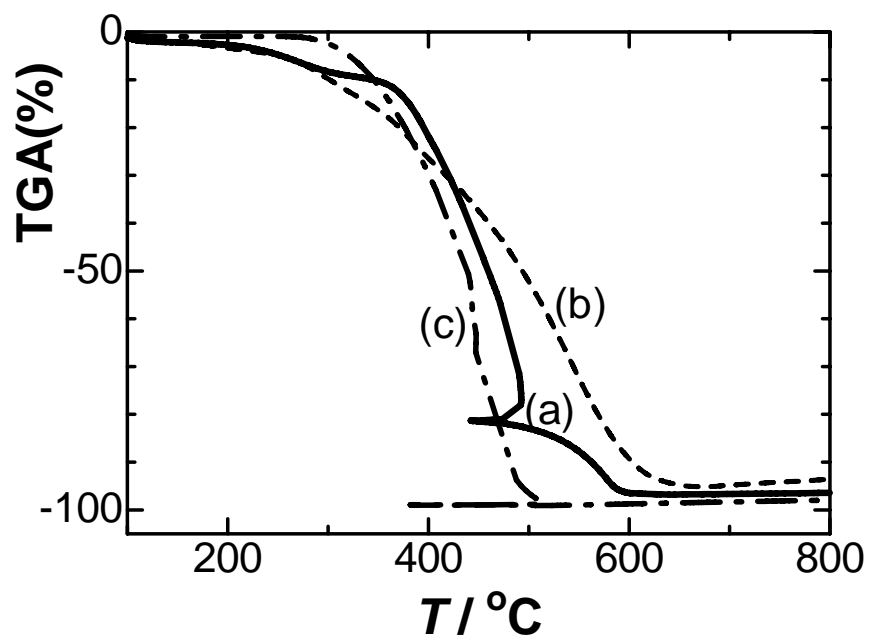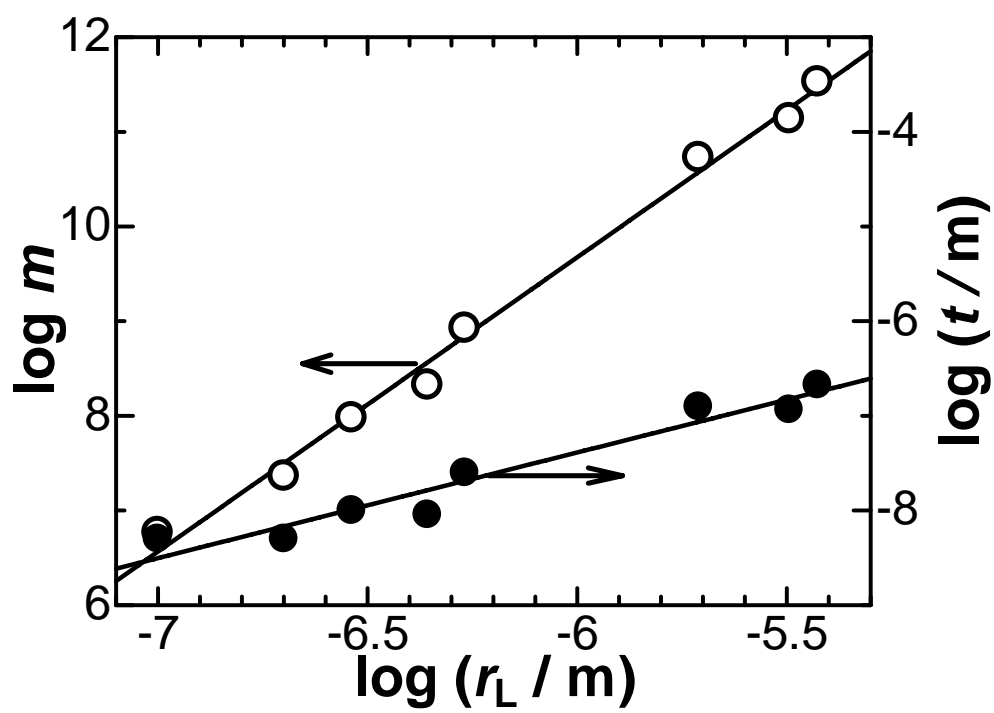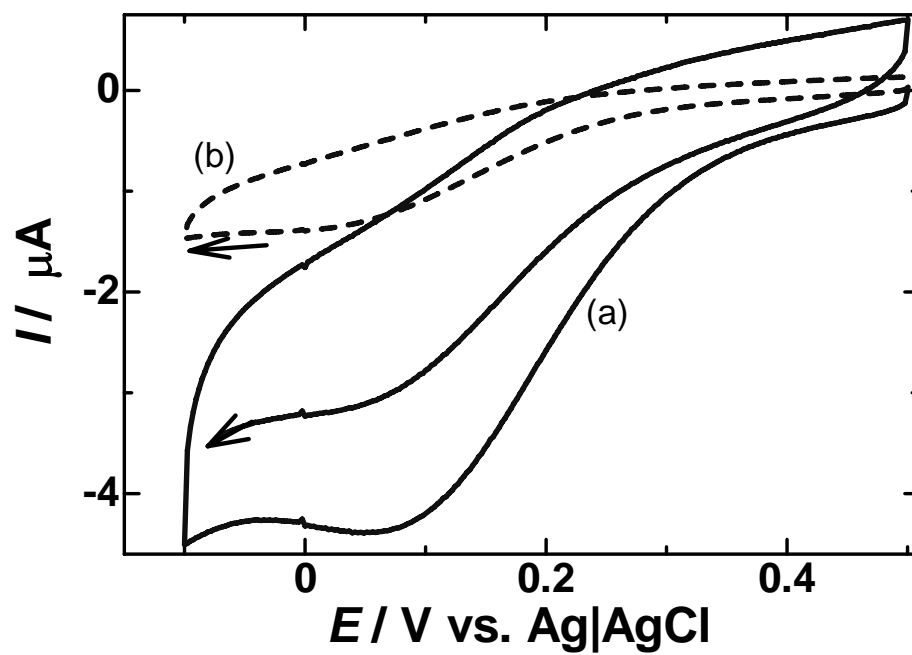
Size Distribution by Intensity

Fig.1(A)

Fig.1(B)

Fig.2

Fig. 3

Fig. 4
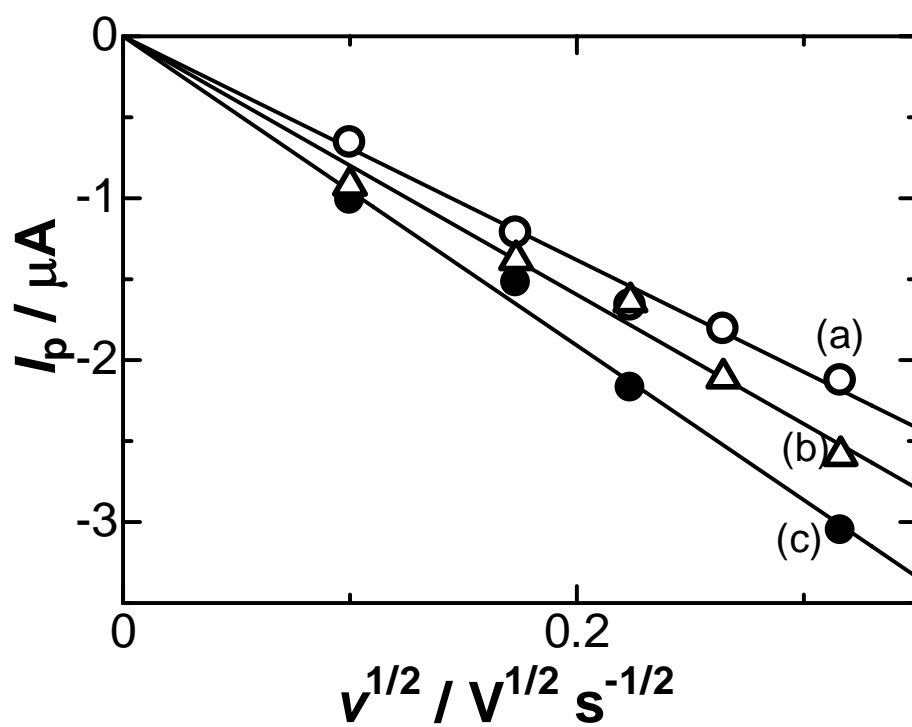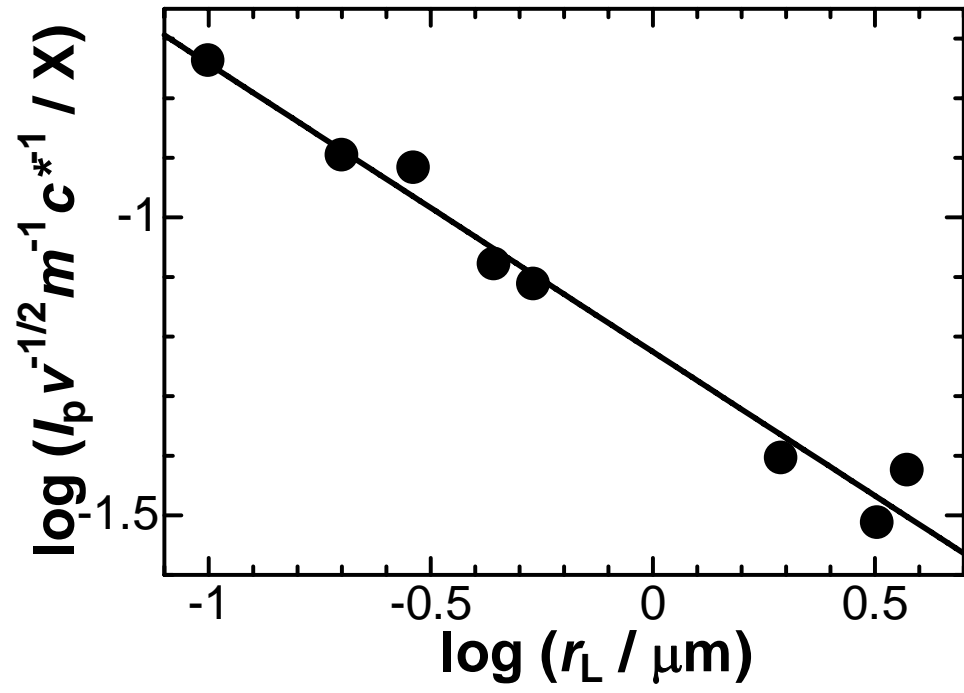

Fig.5

Fig.6.

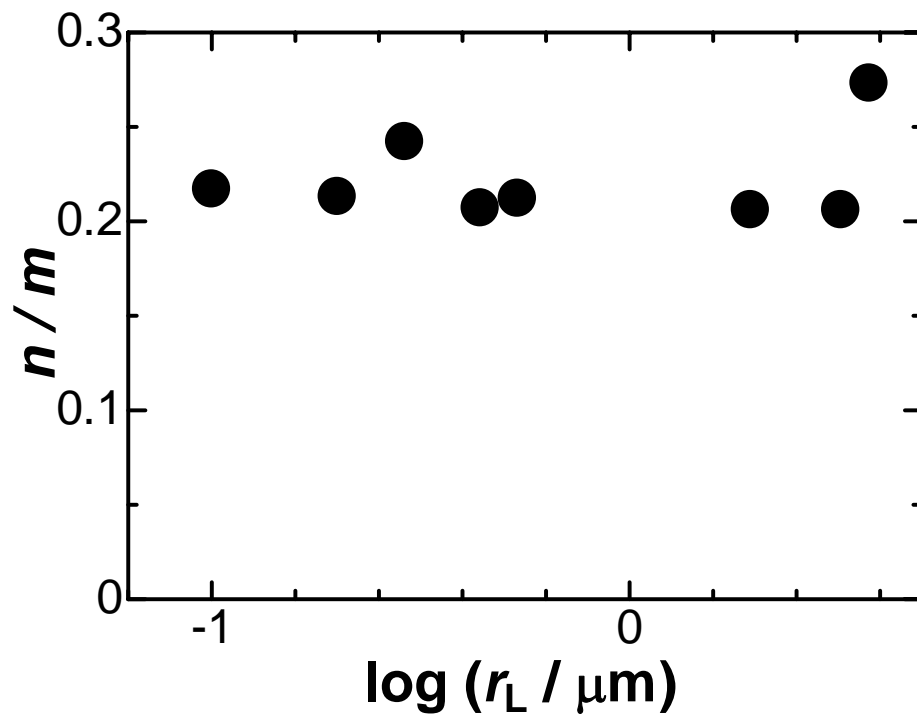
Fig.7.

Fig. 8

Table 1. Conditions of polymerization of polystyrene latexes

	$V(E)$ / cm^3	$V(W)$ / cm^3	$V(P)$ / cm^3	$V(M)$ / cm^3	$V(St)$ / cm^3	$W(SDS)$ / g	$W(PVP)$ / g	$W(A)$ / g	rotation speed/rpm	$2r_L$ / μm
1)	0	120	0	0	8	0	1.5	0.15	400	0.20
2)	0	100	20	0	8	0.15	0.0	0.15	400	0.40
3)	0	0	120	0	10	0	1.5	0.15	350	0.58
4)	0	0	120	0	10	0	3.0	0.15	350	0.89
5)	40	0	0	36	15	0	1.5	0.33	160	1.08
6)	18	0	0	12	5	0	0.8	0.08	120	3.90
7)	18	0	0	12	5	0	0.5	0.11	120	6.41
8)	18	0	0	12	10	0	0.5	0.25	120	7.50

E: ethanol, W: water, P: 2-propanol, M: methoxyethanol, St: styrene, A: AIBM

Table 2. Amount of PANI loaded on one particle

	$2\,r_L$ / μm	W_{PS}/W_{PA} WA	W_{PS}/W_{PA} TGA	r_a/r_L	t / nm	m	$D \times 10^9$/ cm^2 s^{-1}
1)	0.20	4.35	4.44	0.050	5	5.9×10^6	24
2)	0.40	9.38	7.82	0.024	5	2.3×10^7	12
3)	0.58	6.47	3.49	0.035	10	9.6×10^7	8.5
4)	0.89	10.7	1.31	0.021	9	2.1×10^8	5.6
5)	1.08	4.65	5.10	0.047	25	8.4×10^8	4.5
6)	3.90	3.26	3.43	0.064	125	5.4×10^{10}	1.3
7)	6.41	6.15	7.77	0.036	116	1.4×10^{11}	0.76
8)	7.50	3.76	4.91	0.057	212	3.4×10^{11}	0.65

References

[1] Y. M. Abu, K. Aoki, J. Electroanal. Chem. 565 (2003) 219.

[2] Y. M. Abu, K. Aoki, Electrochim. Acta 50 (2005) 3634.

[3] X. G. Li, M. R. Huang, J. F. Zeng, M. F. Zhu, Colloid. Surf. A 248 (2004) 111.

[4] Y. M. Abu, K. Aoki, J. Electroanal. Chem. 583 (2005) 133.

[5] H. Sun, N. Hu, J. Electroanal. Chem. 588 (2006) 207.

[6] Y. Zhou, Z. Li, N. Hu, Y. Zeng, J. F. Rusling, Langmuir 18 (2002) 8573.

[7] J. M. Roberts, P. Linse, J. G. Osteryoung, Langmuir 14 (1998) 204.

[8] K. Aoki, T. Lei, Electrochem. Commun. 1 (1999) 101.

[9] K. Aoki, J. M. Roberts, J. G. Osteryoung, Langmuir, 14, (1998) 4445.

[10] K. Aoki, C. Wang, Langmuir 17 (2001) 7371.

[11] C. Xu, K. Aoki, Langmuir 20 (2004) 10194.

[12] J. Chen, Z. Zhang, J. Electroanal. Chem. 583 (2005) 116.

[13] L. Han, J. Chen, K. Aoki, J. Electroanal. Chem. 602 (2007) 123.

[14] Y. Gao, J. Chen, J. Electroanal. Chem. 578 (2005) 129.

[15] Y. Gao, J. Chen, J. Electroanal. Chem. 583 (2005) 286.

[16] R. B. Bjorklung, S. P. Armes, S. Maeda, S. Y. Luk, J. Colloid Interface Sci. 197 (1998) 179.

[17] K. Aoki, Q. Ke, J. Electroanal. Chem. 587 (2006) 86.

[18]A. Sevcik, Coll. Czech. Chem. Commun. 13 (1948) 349.

[19] R. S. Nicholson, I. Shain, Anal. Chem. 36 (1964) 706.

[20] W. H. Reinmuth, J. Am. Chem. Soc. 79 (1957) 6358.

[21] K. Aoki, Electroanalysis, 17 (2005) 1379.

[22] I. Jureviciute, S. Bruckenstein, A. R. Hillman, J. Electroanal. Chem. 488 (2000) 73.

[23] J. Chen, C. Xu, K. Aoki, J. Electroanal. Chem. 546 (2003) 79.

[24] C. Xu, J.Chen, K.Aoki, Electrochem. Commun. 5 (2003) 506.

[25] K. Aoki, Electrochim. Acta 51 (2006) 6012.

[26] K. Aoki, J. Electroanal. Chem. 310 (1991) 1.

[27] K. Aoki, J. Cao, Y. Hoshino, Electrochim. Acta 38 (1993) 1711.

[28] K. Aoki, M. Kawase, J. Electroanal. Chem. 377 (1994) 125.

[29] K. Aoki, J. Electroanal. Chem. 373 (1994) 67.

[30] J. C. Lacroix, K. Fraoua, P. C. Lacaze, J. Electroanal. Chem. 444 (1998) 83.

[31] K. Aoki, Y. Tezuka, J. Electroanal. Chem. 267 (1989) 55.

[32] Y. Tezuka, K. Aoki, J. Electroanal. Chem. 273 (1989) 161.

[33] Y. Tezuka, S. Ohyama, T. Ishii, K. Aoki, Bull. Chem. Soc. Jpn. 64 (1991) 2045.

[34] K. Aoki, T. Aramoto, Y. Hoshino, J. Electroanal. Chem. 340 (1992) 127.

[35] K. Aoki, J. Chen, Q. Ke, S. P. Armes, D. P. Randall. Langmuir 19 (2003) 5511.

[36] T. Lei, K. Aoki, J. Electroanal. Chem. 482 (2000) 149

[37] A. W. Adamson, Physical Chemistry of Surfaces, 3rd edition, John Wiley & Sons, New York, 1976, pp. 4-10.

[38] K. Aoki, T. Edo, J. Cao, Electrochim. Acta, 43 (1997) 285.

[39] W. -S. Huang, B. D. Humphrey, A. G. MacDiarmid, J. Chem. Soc. Faraday Trans. 82 (1986) 2385.

[40] K. Aoki, J. Electroanal. Chem. 373 (1994) 67.

[41] K. Aoki, M. Kawase, J. Electroanal. Chem. 377 (1994) 125.

[42] K. Aoki, J. Cao, Y. Hoshino, Electrochim. Acta 39 (1994) 2291.

[43] Y. Tezuka, T. Kimura, T. Ishii, K. Aoki, J. Electroanal. Chem. 395 (1995) 51.

[44] J. Cao, K. Aoki, Electrochim. Acta 41 (1996) 1787.

[45] B. Villeret, M. Nechtschein, Phys. Rev. Lett. 63 (1989) 1285.

[46] C. Odin, M. Nechtschein, Phys. Rev. Lett. 67 (1991) 1114.